

基于卟啉小分子给体与双组分富勒烯受体的高效三元有机太阳能电池

孙延娜 高欢欢 张雅敏 王云闯 阚斌 万相见
张洪涛 陈永胜*(*南开大学化学学院 元素有机化学国家重点实验室 纳米科学与技术研究中心
功能高分子材料重点实验室 天津 300071)

摘要 最近,有机太阳能电池中三元策略的出现使得高能量转化效率和简便的器件制备方式有望同时实现.大量实验证明,通过构造三元有机太阳能电池可以实现吸光互补以提高电流或者在能级间形成级联以提高开压.设计并合成了以并噻吩取代卟啉为核,通过炔键连接二酮吡咯并吡咯末端基团的新分子,命名为 DEP-TT,该分子有较小的能带间隙(1.31 eV),光谱吸收可达 898 nm.以该卟啉分子为给体,富勒烯 PC₇₁BM 为受体制备双组分有机太阳能电池,效率可达 7.46%,但开压相对较低(0.75 V).进一步研究发现,加入 10%的富勒烯衍生物 ICBA 制备三元有机太阳能电池,效率可增大至 8.15%,这是基于卟啉小分子为给体的有机太阳能电池取得相对高效率的器件之一.由于 PCBM 和 ICBA 两组分间形成级联能级和协同作用,器件效率明显提高,这意味着三元有机太阳能电池的构建可以同时提高开压和电流,从而实现器件效率的全面提高.

关键词 卟啉小分子给体;双组分富勒烯受体;三元有机太阳能电池

An Efficient Ternary Organic Solar Cell with a Porphyrin Based Small Molecule Donor and Two Fullerene Acceptors

Sun, Yanna Gao, Huanhuan Zhang, Yamin Wang, Yunchuang Kan, Bin
Wan, Xiangjian Zhang, Hongtao Chen, Yongsheng*

(* State Key Laboratory of Element-Organic Chemistry, Centre of Nanoscale Science and Technology and Key Laboratory of Functional Polymer Materials, College of Chemistry, Nankai University, Tianjin 300071)

Abstract Recently, ternary organic solar cells have emerged as a promising strategy to achieve both high performance and fabrication simplicity for organic solar cells. It has been proved that this strategy is an effective way to achieve improved short-circuit current density (J_{sc}) with complementary absorption or to get enhanced open-circuit voltage (V_{oc}) through forming energy level cascade. In this work, we designed and synthesized a thieno[3,2-*b*]thiophene-substituted porphyrin molecule flanked with two diketopyrrolopyrrole units by ethynylene bridges, named DEP-TT, which exhibited a very low energy bandgap of 1.31 eV and a broad light absorption to 898 nm. The power conversion efficiency (PCE) of binary devices based on DEP-TT and the acceptor [6,6]-phenyl-C₇₁-butyric-acid-methyl-ester (PC₇₁BM) achieved 7.46% with a relatively low V_{oc} of 0.75 V. Furthermore, the ternary solar cells with 10% indene-C₆₀ bis-adduct (ICBA) achieved high PCE of 8.15%, with higher V_{oc} , J_{sc} and a relatively higher PCE based on organic solar cells with a porphyrin-small molecule as the donor. This improved performance is believed to be due to the energy level cascade and synergistic effects of the two acceptors of PCBM and ICBA, which suggests that the ternary bulk heterojunction (BHJ) strategy is a promising way to improve both V_{oc} and J_{sc} simultaneously and thus overall performance for the same donor material.

Keywords porphyrin small molecule donor; two fullerene acceptors; ternary organic solar cell

In the past decade, great efforts have been devoted on the organic solar cells (OSCs).^[1-6] Recently, power con-

version efficiencies (PCEs) of over 12% have been achieved based on single junction organic solar cells due to

* Corresponding author. E-mail: yschen99@nankai.edu.cn

Received June 19, 2017; revised July 19, 2017; published online August 30, 2017.

Dedicated to Professor Yangjie Wu on the occasion of his 90th birthday.

Project supported by the Ministry of Science and Technology (No. 2014CB643502), the National Natural Science Foundation of China (Nos. 51373078, 51422304, 91433101) and the Natural Science Foundation of Tianjin City (No. 17JCZDJC31100).

科技部(No. 2014CB643502)、国家自然科学基金(No. 51373078, 51422304, 91433101)和天津市自然科学基金(No. 17JCZDJC31100)资助项目.

the evolution of novel donor materials including polymer and small-molecule, and device optimization.^[7–23] However, further improvement of the single junction OSCs is limited by two factors. One is the insufficient absorption of the active layers and another is the trade-off of the V_{oc} and J_{sc} when low band gap materials with broad absorption are used for harvesting more photons.^[24–27] Although the tandem cell strategy could offset the above problems, efficient subcells with matched absorption and complicated fabrication techniques are needed.^[28–32] As an alternative approach, the ternary-blend structure organic solar cells in which either two donors and one acceptor or one donor and two acceptors as the active layer materials have attracted much more attention owing to its advantages of combining the simplicity of binary structure and complementary optical absorption from tandem devices. It has been proved that the ternary structure strategy is an effective way to achieve improved J_{sc} with complementary absorption^[33–40] or to get enhanced V_{oc} through forming energy level cascade.^[41–45]

It is well known that porphyrins have strong absorptions, unique electronic and redox properties due to their large delocalized π -conjugated system.^[46] Polymers or small molecules incorporating porphyrin units have shown great potential in the OSC applications.^[47] Recently, Peng *et al.* reported a series of porphyrin based small molecules as donor materials and obtained PCEs of 7%~9%.^[48–51] Although with low energy loss, the above porphyrin based small molecules still suffer the low V_{oc} in contrast to other small molecules due to their relatively high HOMO.^[12] For bulk-heterojunction OSCs, the V_{oc} is usually correlate with the difference between the lowest unoccupied molecular orbital (LUMO) energy level of the acceptor and the highest occupied molecular orbital (HOMO) energy level of the donor. Introduction of the second acceptor materials with high LUMO to form ternary active layers might be an effective way to increase the V_{oc} .^[52–54] Meanwhile, high device performances could be expected through device optimization without sacrificing the J_{sc} or with improved J_{sc} or fill factor (FF) due to forming the energy level cascade and synergistic effects.^[35,44]

In this work, we designed and synthesized a thieno-[3,2-*b*]thiophene-substituted porphyrin molecules flanked with two diketopyrrolopyrrole units by ethynylene bridges, namely DEP-TT (Scheme 1). This material exhibited a very low energy bandgap of 1.31 eV and a broad light absorption to 898 nm. The DEP-TT:PC₇₁BM binary blend active film based devices gave a PCE of 7.46% with an open-circuit voltage (V_{oc}) of 0.75 V. When indene-C60 bis-adduct (ICBA) with higher LUMO (−3.70 eV, Figure 1c) as the second acceptor was introduced, a PCE of 8.15% with improved V_{oc} and J_{sc} was achieved. These results demonstrated that ternary active layer by introduction of higher LUMO acceptor is an effective strategy to improve the device performance of low band gap materials.

1 Results and discussion

1.1 Synthesis and characterization

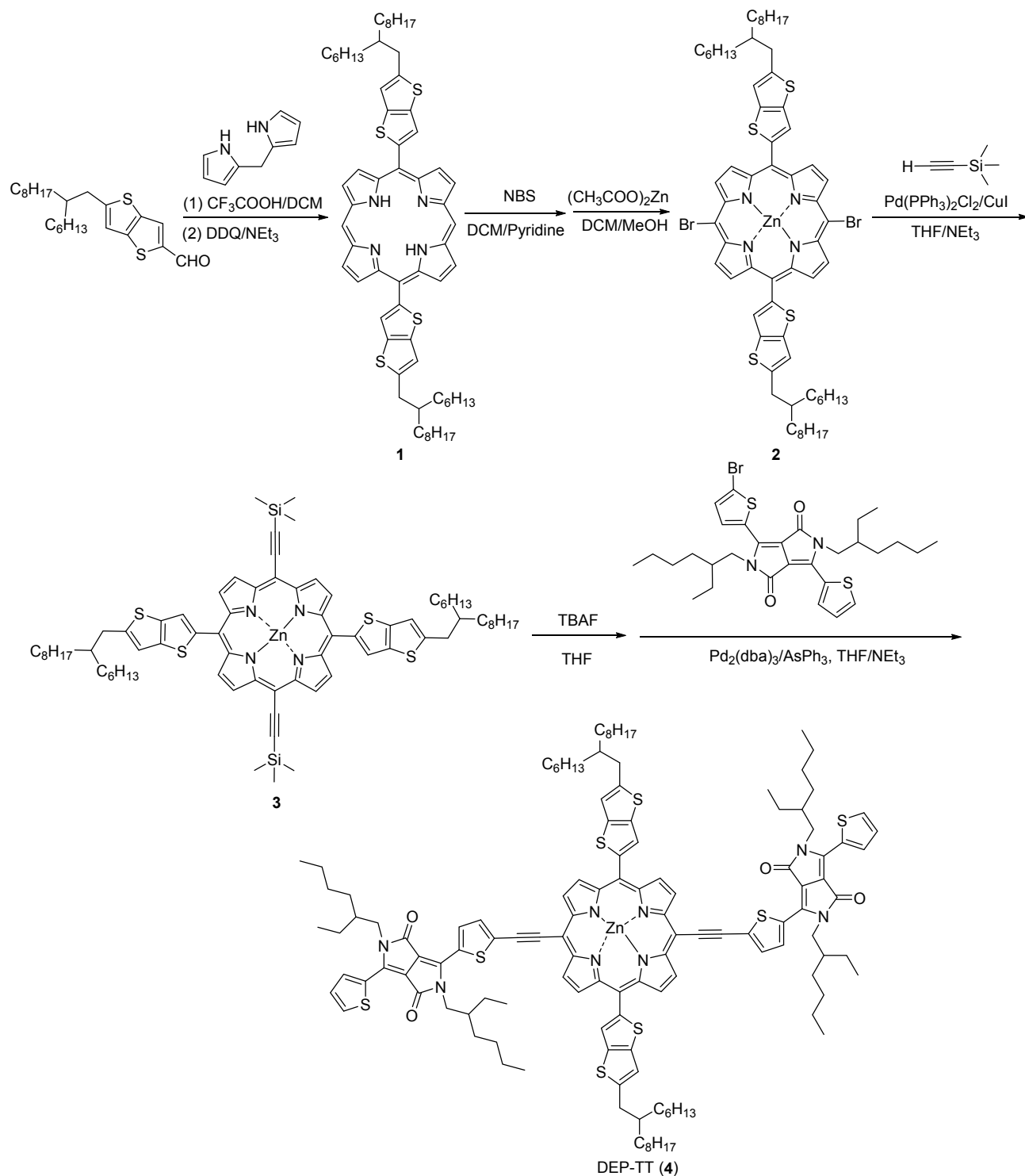
The target molecule 5,15-Bis(2,5-bis-(2-ethyl-hexyl)-3,6-di-thienyl-2-yl-2,5-dihydro-pyrrolo[3,4-*c*]pyrrole-1,4-dione-5'-yl-ethynyl)-10,20-bis(5-(2-hexyldecyl)-thieno[3,2-*b*]thienyl)porphyrin zinc(II) (DEP-TT) was synthesized by a Sonogashira coupling reaction according to the reported procedures.^[46] The synthesis routes were shown in Scheme 1. The target compound DEP-TT was synthesized in 80% yield and purified by column chromatography on silica gel and fully characterized.

1.2 Optical absorption and electrochemical properties

The absorption spectra of DEP-TT in solution and thin film showed a broad spectral coverage in the visible and near-infrared (NIR) regions as shown in Figure 1b and some important optical data are listed in Table 1. In dilute chloroform solution, three strong absorption peaks at 470, 565, and 724 nm were observed. Such strong absorption in the NIR region at a short backbone length indicates that the π -electron delocalization between constituent units is very effective. In thin film, DEP-TT exhibited red-shifted absorption peaks at 473, 572, and 788 nm with a shoulder peak at 732 nm. While 473 and 572 nm peaks come from the porphyrin Soret band and the absorption of the DPP moiety, the long-wavelength absorption peaks at 732 and 788 nm are attributed to the intramolecular charge transfer and intermolecular π - π stacking, respectively. Moreover, the significant red-shift of 64 nm from 724 nm in solution to 788 nm in film is attributed to the strong intermolecular π - π stacking in the solid state. The optical band gap is calculated to be 1.38 eV based on the onset of the thin film absorption spectrum (898 nm). The HOMO energy level and LUMO energy level are −4.81 and −3.50 eV for DEP-TT estimated from cyclic voltammetry measurements (see the Supporting Information).

1.3 Photovoltaic properties

Solution-processed bulk heterojunction solar cells using DEP-TT as the donor material with a device structure of glass/ITO/PEDOT:PSS/DEP-TT:PC₇₁BM/PrC₆₀MA/Al were fabricated. PrC₆₀MA is a methanol-soluble fullerene-surfactant developed by Alex *et al.* as an efficient interfacial layer for cathodes,^[55] and its structure is shown in Figure 2S. The optimized donor/acceptor weight ratio was 1 : 0.8, and pyridine was used as additive. Typical current density-voltage (J - V) curves of solar cells with different post-treatments and different donor concentrations and the corresponding device parameters were presented in the Supporting Information. With 4% (V/V) pyridine, the device shows a PCE of 3.47%, with a V_{oc} of 0.87 V, a J_{sc} of 9.72 mA·cm^{−2}, and a FF of 0.41. After thermal annealing (TA) at 100 °C for 10 min, the PCE increased to 5.48%. As an effective approach, solvent vapor annealing (SVA) has been used in small molecule based OSCs devices to fine-tune the morphology of the active layer.^[56] Thus, this



Scheme 1 Synthesis routes for DEP-TT

approach was employed in the following device optimization. After TA, the active layer was exposed to chloroform vapour for 90 s, the PCE significantly improved to 7.46%, with an outstanding J_{sc} of $15.31 \text{ mA}\cdot\text{cm}^{-2}$, and a high FF of 0.65, however, these devices exhibited a relatively lower V_{oc} .

As discussed above, although with low energy loss, the porphyrin based small molecule donors still exhibits low

V_{oc} . In order to improved V_{oc} , adding the second acceptor materials with high LUMO to form energy level cascade might be an effective way.^[39,42] Considering the higher LUMO level and the similar chemical structure of ICBA relative to PC_{71}BM , ICBA was introduced to the DEP-TT: PC_{71}BM binary devices to form the ternary solar cells. As shown in Figure 2, we investigated the influence of ICBA with different weight ratios on the performances

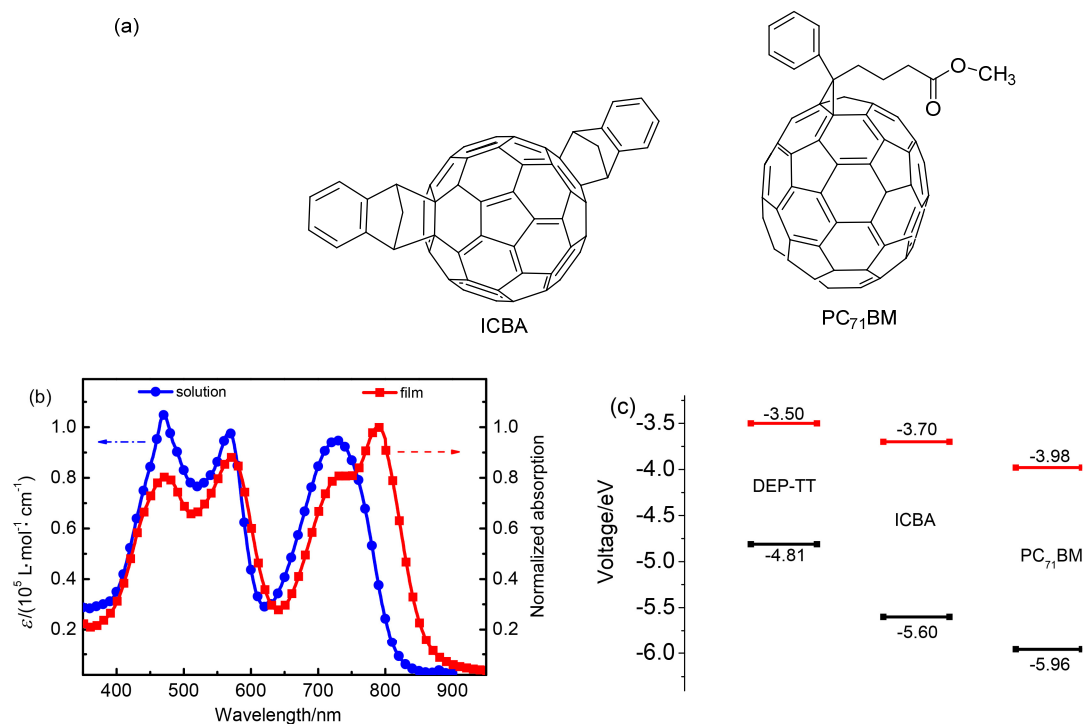


Figure 1 (a) Chemical structures of PC₇₁BM and ICBA; (b) UV-Vis absorption spectra of DEP-TT in chloroform solution and in as-cast film; (c) energy levels of materials used

Table 1 Optical and electrochemical data of DEP-TT^a

UV-Vis			CV		
$\lambda_{\max, \text{sol}}/\text{nm}$	$\varepsilon/(10^5 \text{ L}\cdot\text{mol}^{-1}\cdot\text{cm}^{-1})$	$\lambda_{\max, \text{film}}/\text{nm}$	HOMO/eV	LUMO/eV	$E_g^{\text{cv}}/\text{eV}$
470	1.045	473	-4.81	-3.50	1.31
565	0.978	572			
724	0.946	732			
		788			

^aHOMO and LUMO are estimated from cyclic voltammetry measurements referenced by the energy level of Fc/Fc⁺ (-4.4 eV below vacuum).

of the ternary device. As we expected, the V_{oc} was improved linearly with increasing ICBA content, gradually increased from 0.75 V to 0.87 V with the ICBA content from 0 to 100%. However, the J_{sc} , FF and PCE demonstrate a different relationship with the ICBA ratios. At low ICBA ratios, the three parameters are less sensitive to the ICBA content when the ICBA content is below 20%. But they decrease significantly while further increasing of ICBA content from 20% to 100%. Figure 3b shows the J - V curves in OSCs with three different representative ICBA contents. Thus, the optimized PCE of 8.15% is achieved for the ternary organic solar cells (OSCs) with 10% ICBA content with improved V_{oc} , J_{sc} and FF due to forming the energy level cascade and synergistic effects. Detailed photovoltaic parameters are also listed in Table 2.

Figure 3a exhibits that with low increasing content of ICBA, the DEP-TT:PC₇₁BM:ICBA films show nearly the same absorption profiles, which indicates that the introduction of small amount ICBA does not interrupt much the packing modes of the donor molecules. As shown in Figure 3c, the trend of EQE with different ICBA loading is similar to that of J_{sc} . The J_{sc} values integrated from the

EQE curves were 15.09, 15.27, 12.79 mA·cm⁻², corresponding to the ICBA 0%, 10%, 50% device respectively, which are consistent with the data from the J - V curves (the average error is less than 5% mismatch). The improvement of the J_{sc} might be due to the slightly improved morphology as discussed below.

1.4 Morphology

As reported in previous studies, the addition of a third component into a binary BHJ blend would affect its phase separation morphology.^[25,46] Thus, the performance of ternary OSCs is closely related to the contents of the third component. To investigate the influence of the third component on the film morphology in ternary blends, we investigated the phase-separation morphologies of the blends by tapping-mode atomic force microscopy (AFM) and transmission electron microscopy (TEM), as shown in Figure 4. Smaller domain sizes and more smooth surfaces were observed in DEP-TT:PC₇₁BM:ICBA films than the DEP-TT:PC₇₁BM films and the RMS roughness significantly decreases from 1.39 nm to 0.556 nm with the contents of ICBA increasing from 0 to 100%. From the TEM,

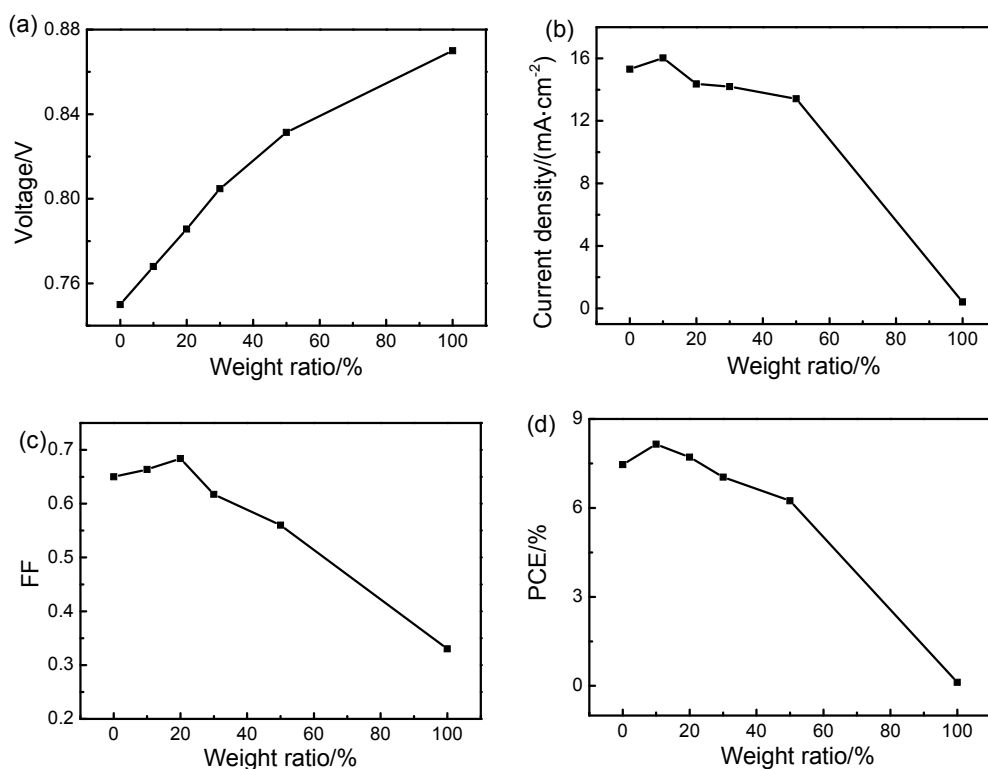


Figure 2 (a) V_{oc} , (b) J_{sc} , (c) FF and (d) PCE based on devices with different ICBA weight ratios in the acceptor

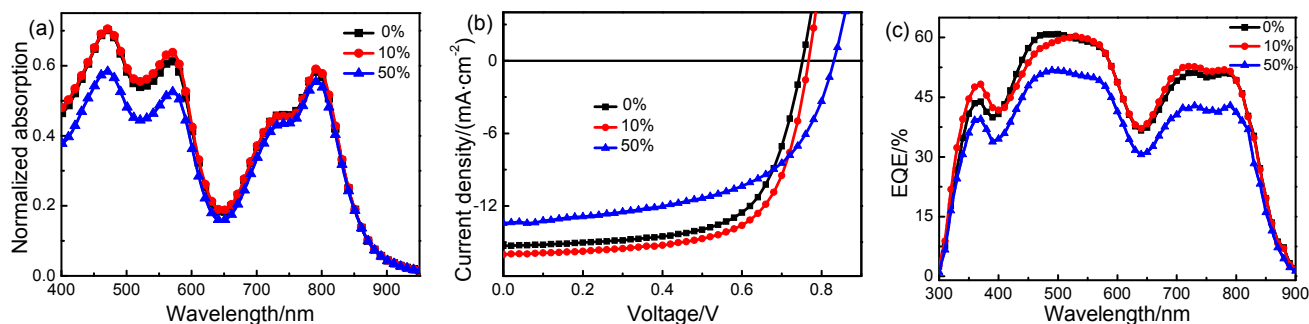


Figure 3 (a) UV-Vis absorption spectra of active-layer materials, (b) J - V curves and (c) EQE based on devices with varying ICBA weight ratios (0%, 10%, 50%) in the acceptor.

Table 2 Summary of solar cell parameters of ternary DEP-TT:PC₇₁BM:ICBA blend with different ICBA content (wt%) in the acceptor^a

ICBA content/%	V_{oc}/V	$J_{sc}/(\text{mA}\cdot\text{cm}^{-2})$	FF	$\text{PCE}_{\text{max}}/\%$	$\text{PCE}^a/\%$
0	0.75	15.31	0.65	7.46	7.42 ± 0.04
5	0.75	15.94	0.65	7.82	7.79 ± 0.03
10	0.77	16.03	0.66	8.15	8.06 ± 0.09
20	0.79	14.36	0.68	7.71	7.59 ± 0.12
30	0.80	14.20	0.62	7.04	6.96 ± 0.08
50	0.83	13.42	0.56	6.24	6.22 ± 0.02
100	0.87	0.41	0.33	0.12	0.11 ± 0.01

^a The average PCE values were calculated from ten devices for each condition.

it can be seen that the film with 10% ICBA (Figure 4e) shows much more obvious nanofiber and interpenetrating structures in contrast to the films without and with ICBA content 50%. Consequently, the ternary blend film could form well-mixed aggregated domains to effectively transport electrons with bicontinuous interpenetrating networks.

2 Conclusions

In summary, we have fabricated a ternary OSC with DEP-TT as the donor, PC₇₁BM and ICBA as the acceptors. A PCE of 8.15% was achieved for the ternary devices with 10% ICBA content, which was enhanced by 9% compared with the binary OSCs based on DEP-TT:PC₇₁BM. Due to the higher LUMO energy levels of ICBA compared to PC₇₁BM, the V_{oc} of the ternary device increases with the

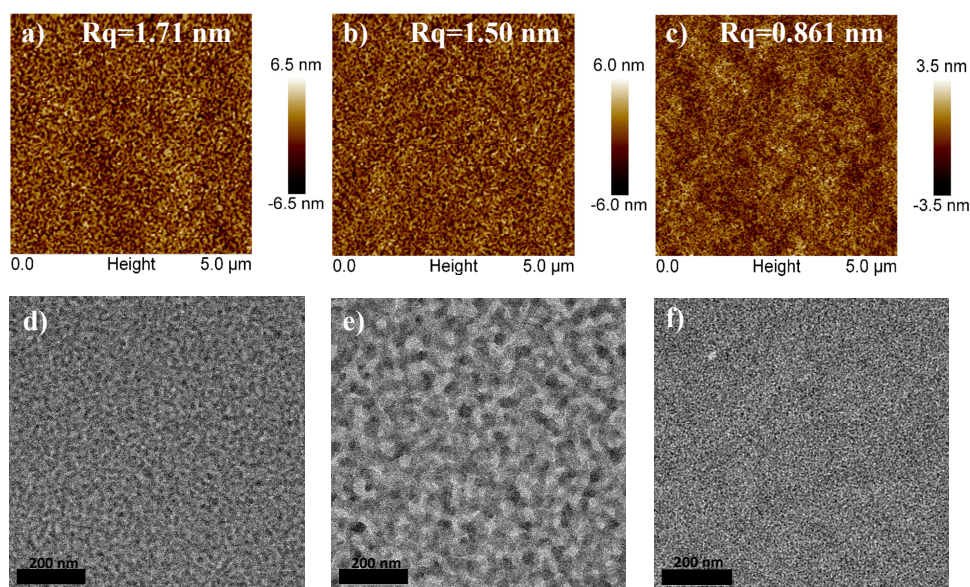


Figure 4 AFM topography (a, b, and c) and TEM images (d, e and f) of DEP-TT:PC₇₁BM:ICBA blend films with varying ICBA content (0%, 10% and 50%) in the acceptor

improved contents of ICBA. It is believed that the overall improved performance of the ternary devices compared with the binary devices is contributed to the synergistic effects of improved V_{oc} and J_{sc} without sacrificing the FF due to forming the energy level cascade and favorable active layer morphology. The results demonstrate that the ternary BHJ strategy is a promising way to develop high efficiency OSCs since the synergistically improved photovoltaic parameters such as V_{oc} and J_{sc} can be attained through dedicate component design and selection, and morphology control.

3 Experimental section

3.1 Instruments and reagents

Instruments includes Keithley 2400 source-measure unit, Axen-on-lamp-based solar simulator [SAN-EI XES-70S1(AM 1.5G)], Stanford Research Systems SR810 lock-in amplifier, JASCO V-570 spectrophotometer, LK98B II microcomputer-based Electrochemical Analyzer, MultiMode 8 atomic force microscope, Philips Technical G2 F20 at 200 kV. All reagents and solvents were purchased from the commercial corporation and used without further purification.

3.2 Synthesis and characterization

5,15-Bis(5-(2-hexyldecyl)-thieno[3,2-*b*]thienyl)-porphyrin (1): A solution of 5-(2-hexyldecyl)-thieno[3,2-*b*]thiophene-2-carbaldehyde (1.60 g, 4.075 mmol) and dipyrromethane (596 mg, 4.075 mmol) in dichloromethane (DCM) (800 mL) was purged with argon for 30 min, and then trifluoroacetic acid (TFA) (0.27 mL) was added. The mixture was stirred for 12 h at room temperature, and then 2,3-dichloro-5,6-dicyano-1,4-benzoquinone (DDQ) (1.38 g) was added. After the mixture was stirred at room temperature for an additional 2 h, the reaction was quenched

by triethylamine (5 mL). Then the solvent was removed under reduced pressure, and the residue was purified by flash column chromatography on silica gel using dichloromethane/petroleum ether ($V/V=1/2$) as the eluent. Recrystallization from DCM/methanol (MeOH) gave **1** as a purple solid. m.p. 202~205 °C; ¹H NMR (400 MHz, CDCl₃) δ : 10.25 (s, 2H), 9.40 (d, $J=4.6$ Hz, 4H), 9.35 (d, $J=4.6$ Hz, 4H), 8.03 (s, 2H), 7.21 (s, 2H), 3.03 (d, $J=6.6$ Hz, 4H), 1.84~1.91 (m, 2H), 1.52~1.45 (m, 14H), 1.41~1.33 (m, 34H), 0.95 (m, 12H), -3.01 (s, 2H); ¹³C NMR (101 MHz, CDCl₃) δ : 148.06, 147.28, 145.40, 141.71, 141.44, 137.33, 131.82, 131.13, 126.15, 117.11, 111.14, 106.10, 40.19, 35.80, 33.36, 31.99, 30.08, 29.76, 29.73, 29.41, 26.73, 22.75, 14.19, 14.17. HR-MS (MALDI) calcd for C₆₄H₈₂N₄S₄ 1034.5422, found 1034.5424.

5,15-Dibromo-10,20-bis(5-(2-hexyldecyl)-thieno[3,2-*b*]thienyl)-porphyrin zinc(II) (2): Porphyrin **1** (820 mg, 0.792 mmol) and pyridine (5 mL) were dissolved in 150 mL of dichloromethane. Then *N*-bromosuccinimide (NBS) (310 mg, 1.742 mmol) was added and the mixture was stirred at room temperature for another 2 h. Then the reaction was quenched by 5 mL of acetone, and the mixture was washed with water and dried over anhydrous Na₂SO₄. After the solvent was removed, the residue was purified by flash column chromatography on silica gel using petroleum ether/DCM ($V/V=3/1$) as the eluent. Recrystallization from DCM/MeOH gave a purple solid. To a solution as mentioned above (500 mg, 0.419 mmol) in chloroform (80 mL), was added a solution of Zn(OAc)₂·2H₂O (460 mg, 2.095 mmol) in MeOH (10 mL). The reaction mixture was stirred at room temperature for 2 h and then washed with water and dried over anhydrous Na₂SO₄. After the solvent was removed, the residue was recrystallized from DCM/methanol to afford a dark green solid **2**. m.p. 148~153 °C. ¹H NMR (400 MHz, CDCl₃) δ : 9.29 (d, $J=4.6$

Hz, 4H), 9.00 (d, $J=4.2$ Hz, 4H), 7.80 (s, 2H), 7.15 (s, 2H), 3.02 (s, 4H), 1.92~1.81 (m, 2H), 1.51~1.44 (m, 14H), 1.42~1.33 (m, 32H), 0.99~0.91 (m, 14H); ^{13}C NMR (101 MHz, CDCl_3) δ : 151.33, 149.86, 147.28, 142.10, 141.02, 136.87, 133.29, 132.99, 126.08, 116.96, 113.58, 105.63, 40.18, 35.79, 33.34, 32.03, 32.00, 30.11, 29.78, 29.76, 29.43, 26.73, 22.78, 22.76, 14.22, 14.19. HR-MS (MALDI) calcd for $\text{C}_{64}\text{H}_{78}\text{Br}_2\text{N}_4\text{S}_4\text{Zn}$ 1252.2768, found 1252.2768.

5,15-Bis(trimethylsilyl)ethyl-10,20-bis(5-(2-hexyldecyl)-thieno[3,2-*b*]thienyl)-porphyrin zinc(II) (**3**): Porphyrin **2** (720 mg, 0.573 mmol) was dissolved in THF (40 mL) and triethylamine (8 mL) was added. The mixture was purged with argon for 30 min. Then $\text{Pd}(\text{PPh}_3)_2\text{Cl}_2$ (40 mg, 0.0573 mmol), CuI (11 mg, 0.0573 mmol), and trimethylsilylacetylene (281 mg, 2.865 mmol) were added. The mixture was stirred at room temperature for 12 h under argon, and then the reaction was quenched with saturated brine. After the mixture was extracted with dichloromethane a few times, the combined organic layers were dried with anhydrous Na_2SO_4 and concentrated. Finally, the residue was purified by column chromatography (silica gel, DCM/petroleum ether ($V/V=1/2$)) to afford **3** as a green solid. m.p. 55~60 °C; ^1H NMR (400 MHz, CDCl_3) δ : 9.63 (d, $J=4.6$ Hz, 4H), 9.22 (d, $J=4.6$ Hz, 4H), 7.97 (s, 2H), 7.18 (s, 2H), 3.02 (d, $J=6.6$ Hz, 4H), 1.90~1.83 (m, 2H), 1.50~1.43 (m, 14H), 1.40~1.32 (m, 32H), 1.01~0.88 (m, 14H), 0.61 (s, 18H); ^{13}C NMR (101 MHz, CDCl_3) δ : 152.10, 150.77, 146.88, 142.06, 140.69, 136.64, 132.52, 131.18, 125.64, 116.71, 114.03, 106.63, 102.07, 101.90, 39.86, 35.46, 33.04, 31.70, 31.68, 29.77, 29.45, 29.42, 29.10, 26.41, 22.45, 22.44, 13.88, 13.87. HR-MS (MALDI) calcd for $\text{C}_{74}\text{H}_{96}\text{N}_4\text{S}_4\text{Si}_2\text{Zn}$ 1288.5348, found 1288.5348.

5,15-Bis(2,5-bis(2-ethyl-hexyl)-3,6-di-thienyl-2-yl)-2,5-dihydro-pyrrolo[3,4-*c*]pyrrole-1,4-dione-5'-yl-ethynyl)-10,20-bis(5-(2-hexyldecyl)-thieno[3,2-*b*]thienyl)-porphyrin zinc(II) (**4**): Tetrabutylammonium fluoride (1.75 mL, 1 mol/L in THF) was added to a stirred solution of porphyrin **3** (670 mg, 0.584 mmol) in THF (40 mL). After the mixture was stirred for 15 min, 5 mL of water was added to quench the reaction. Then the solution was extracted with chloroform and dried over anhydrous Na_2SO_4 . After evaporation of the solvent, the residue was purified by column chromatography (silica gel, CHCl_3 /petroleum ether ($V/V=3/1$)) to give a deep blue needle crystals. To a 50 mL two necked round-bottom flask were added 5,15-diethynyl-10,20-bis(5-(2-hexyldecyl)-thieno[3,2-*b*]thienyl)-porphyrin zinc (80 mg, 0.0697 mmol), 3-(5-bromothiophen-2-yl)-2,5-bis(2-ethylhexyl)-6-(thiophen-2-yl)-pyrrolo[3,4-*c*]pyrrole-1,4(2*H*,5*H*)-dione (126 mg, 0.209 mmol), anhydrous THF (12 mL) and triethylamine (3 mL), and the mixture was deoxygenated with argon for 30 min before $\text{Pd}_2(\text{dba})_3$ (6 mg, 0.00655 mmol) and AsPh_3 (42 mg, 0.139 mmol) were added. Then the mixture was stirred at 60 °C for 24 h under the protection of argon. After cooled to room temperature, the mixture was washed with water and dried

over anhydrous Na_2SO_4 . Then the solvent was removed, and the residue was purified first by column chromatography on silica gel to give a black solid DEP-TT. m.p. 112~118 °C; ^1H NMR (400 MHz, $\text{CDCl}_3/\text{DMSO}-d_6$) δ : 9.03 (s, 4H), 8.90 (d, $J=18.9$ Hz, 4H), 8.87~8.79 (m, 2H), 8.77~8.69 (m, 2H), 8.23~8.16 (m, 2H), 7.78~7.72 (m, 2H), 7.38~7.25 (m, 6H), 4.02~3.89 (m, 4H), 3.61~3.56 (m, 4H), 3.20~3.11 (m, 4H), 2.02~1.96 (m, 2H), 1.90~1.84 (m, 2H), 1.82~1.76 (2H), 1.64~1.53 (m, 15H), 1.48~1.24 (m, 65H), 1.03~0.86 (m, 36H). HR-MS (MALDI) calcd for $\text{C}_{128}\text{H}_{156}\text{N}_8\text{O}_4\text{S}_8\text{Zn}$ 2188.9307, found 2188.9308.

3.3 BHJ-OSC devices fabrication

Solar cells based on DEP-TT:PC₇₁BM:ICBA ternary blend with various ICBA contents were fabricated with a device configuration of ITO/PEDOT:PSS/ternary BHJ blend/PrC₆₀MA/Al. PC₇₁BM (purity > 99.0%) was purchased from American Dye Inc. The indium tin oxide (ITO)-coated glass substrates were cleaned by ultrasonic treatment in detergent, deionized water, acetone, and isopropyl alcohol under ultrasonication for 15 min each and subsequently dried by a nitrogen blow. A thin layer of PEDOT:PSS (Clevios PVP Al 4083, filtered at 0.45 μm) was spin-coated at 3000 r/min onto the ITO surface. After being baked at 150 °C for 20 min, the substrates were transferred into an argon-filled glovebox. The donor materials of DEP-TT and the acceptor material PC₇₁BM and ICBA were dissolved in chloroform to generate 18 mg·mL⁻¹ blend solutions. The weight ratios of ICBA to PC₇₁BM were 0%, 10%, 20%, 30%, 50% and 100%, respectively and with an overall ratio of donor to acceptor ratio kept at 1 : 0.8. In fabrication, an additive pyridine (4%, V/V) was used to optimize the devices, the active layer was sequentially handled with thermal annealing (TA) at 100 °C for 10 min and then exposed to chloroform vapor for 90 s to optimize the morphology. A thin layer of PrC₆₀MA and an 80 nm Al layer were deposited on the active layer under high vacuum ($<2 \times 10^{-4}$ Pa).

3.4 Characterization and measurement

The current density-voltage ($J-V$) curves of photovoltaic devices were obtained by a Keithley 2400 source-measure unit. The photocurrent was measured under illumination simulated 100 mW·cm⁻² AM 1.5G irradiation using a xenon-lamp-based solar simulator [SAN-EI XES-70S1 (AM 1.5G)] in an argon filled glove box. External quantum efficiencies (EQE) were measured using Stanford Research Systems SR810 lock-in amplifier. UV-Vis spectra were obtained with a JASCO V-570 spectrophotometer. Cyclic voltammetry (CV) experiments were performed with a LK98B II microcomputer-based Electro-chemical Analyzer. All CV measurements were carried out at room temperature with a conventional three-electrode configuration employing a glassy carbon electrode as the working electrode, a saturated calomel electrode (SCE) as the reference electrode, and a Pt wire as the counter electrode. Dichloromethane was distilled from calcium hydride under

dry nitrogen immediately prior to use. Tetrabutylammonium phosphorus hexafluoride (Bu_4NPF_6 , 0.1 mol/L) in dichloromethane was used as the supporting electrolyte; the scan rate was $100 \text{ mV}\cdot\text{s}^{-1}$. Atomic force microscope (AFM) was performed using MultiMode 8 atomic force microscope in tapping mode. The transmission-electron microscope (TEM) investigation was performed on Philips Technical G² F20 at 200 kV.

Supporting Information Details of device fabrication and characterization. The Supporting Information is available free of charge via the Internet at <http://sioc-journal.cn>.

References

- [1] Heeger, A. J. *Chem. Soc. Rev.* **2010**, *39*, 2354.
- [2] Krebs, F. C. *Sol. Energy Mater. Sol. Cells* **2009**, *93*, 394.
- [3] Li, G.; Zhu, R.; Yang, Y. *Nat. Photonics* **2012**, *6*, 153.
- [4] Lu, L.; Zheng, T.; Wu, Q.; Schneider, A. M.; Zhao, D.; Yu, L. *Chem. Rev.* **2015**, *115*, 12666.
- [5] Service, R. F. *Science* **2011**, *332*, 293.
- [6] Zhang, Z.-G.; Li, Y. *Sci. China: Chem.* **2015**, *58*, 192.
- [7] Baran, D.; Ashraf, R. S.; Hanifi, D. A.; Abdelsamie, M.; Gasparini, N.; Rohr, J. A.; Holliday, S.; Wadsworth, A.; Lockett, S.; Neophytou, M.; Emmott, C. J. M.; Nelson, J.; Brabec, C. J.; Amassian, A.; Salleo, A.; Kirchartz, T.; Durrant, J. R.; McCulloch, I. *Nat. Mater.* **2017**, *16*, 363.
- [8] Bin, H.; Gao, L.; Zhang, Z.-G.; Yang, Y.; Zhang, Y.; Zhang, C.; Chen, S.; Xue, L.; Yang, C.; Xiao, M.; Li, Y. *Nat. Commun.* **2016**, *7*, 13651.
- [9] Dai, S.; Zhao, F.; Zhang, Q.; Lau, T.-K.; Li, T.; Liu, K.; Ling, Q.; Wang, C.; Lu, X.; You, W.; Zhan, X. *J. Am. Chem. Soc.* **2017**, *139*, 1336.
- [10] Jin, Y.; Chen, Z.; Dong, S.; Zheng, N.; Ying, L.; Jiang, X.-F.; Liu, F.; Huang, F.; Cao, Y. *Adv. Mater.* **2016**, *28*, 9811.
- [11] Kan, B.; Feng, H.; Wan, X.; Liu, F.; Ke, X.; Wang, Y.; Wang, Y.; Zhang, H.; Li, C.; Hou, J.; Chen, Y. *J. Am. Chem. Soc.* **2017**, *139*, 4929.
- [12] Kan, B.; Li, M.; Zhang, Q.; Liu, F.; Wan, X.; Wang, Y.; Ni, W.; Long, G.; Yang, X.; Feng, H.; Zuo, Y.; Zhang, M.; Huang, F.; Cao, Y.; Russell, T. P.; Chen, Y. *J. Am. Chem. Soc.* **2015**, *137*, 3886.
- [13] Li, S.; Ye, L.; Zhao, W.; Zhang, S.; Mukherjee, S.; Ade, H.; Hou, J. *Adv. Mater.* **2016**, *28*, 9423.
- [14] Li, Z.; Jiang, K.; Yang, G.; Lai, J. Y. L.; Ma, T.; Zhao, J.; Ma, W.; Yan, H. *Nat. Commun.* **2016**, *7*, 13094.
- [15] Lin, Y.; Zhao, F.; Wu, Y.; Chen, K.; Xia, Y.; Li, G.; Prasad, S. K. K.; Zhu, J.; Huo, L.; Bin, H.; Zhang, Z.-G.; Guo, X.; Zhang, M.; Sun, Y.; Gao, F.; Wei, Z.; Ma, W.; Wang, C.; Hodgkiss, J.; Bo, Z.; Inganas, O.; Li, Y.; Zhan, X. *Adv. Mater.* **2017**, *29*, 1604155.
- [16] Liu, T.; Pan, X.; Meng, X.; Liu, Y.; Wei, D.; Ma, W.; Huo, L.; Sun, X.; Lee, T. H.; Huang, M.; Choi, H.; Kim, J. Y.; Choy, W. C. H.; Sun, Y. *Adv. Mater.* **2017**, *29*, 1604251.
- [17] Qiu, N.; Zhang, H.; Wan, X.; Li, C.; Ke, X.; Feng, H.; Kan, B.; Zhang, H.; Zhang, Q.; Lu, Y.; Chen, Y. *Adv. Mater.* **2017**, *29*, 1604964.
- [18] Vohra, V.; Kawashima, K.; Kakara, T.; Koganezawa, T.; Osaka, I.; Takimiya, K.; Murata, H. *Nat. Photonics* **2015**, *9*, 403.
- [19] Yang, Y.; Zhang, Z.-G.; Bin, H.; Chen, S.; Gao, L.; Xue, L.; Yang, C.; Li, Y. *J. Am. Chem. Soc.* **2016**, *138*, 15011.
- [20] Yao, H.; Cui, Y.; Yu, R.; Gao, B.; Zhang, H.; Hou, J. *Angew. Chem.* **2017**, *129*, 3091.
- [21] Zhang, S.; Ye, L.; Zhao, W.; Yang, B.; Wang, Q.; Hou, J. *Sci. China: Chem.* **2015**, *58*, 248.
- [22] Zhao, F.; Dai, S.; Wu, Y.; Zhang, Q.; Wang, J.; Jiang, L.; Ling, Q.; Wei, Z.; Ma, W.; You, W.; Wang, C.; Zhan, X. *Adv. Mater.* **2017**, *29*, 1700144.
- [23] Zhao, J.; Li, Y.; Yang, G.; Jiang, K.; Lin, H.; Ade, H.; Ma, W.; Yan, H. *Nat. Energy* **2016**, *1*, 15027.
- [24] Ameri, T.; Khoram, P.; Min, J.; Brabec, C. J. *Adv. Mater.* **2013**, *25*, 4245.
- [25] An, Q.; Zhang, F.; Zhang, J.; Tang, W.; Deng, Z.; Hu, B. *Energy Environ. Sci.* **2016**, *9*, 281.
- [26] Lu, L.; Kelly, M. A.; You, W.; Yu, L. *Nat. Photonics* **2015**, *9*, 491.
- [27] Yang, Y.; Chen, W.; Dou, L.; Chang, W.-H.; Duan, H.-S.; Bob, B.; Li, G. *Nat. Photonics* **2015**, *9*, 190.
- [28] Huang, F. *Sci. China: Chem.* **2017**, *60*, 433.
- [29] Li, M.; Gao, K.; Wan, X.; Zhang, Q.; Kan, B.; Xia, R.; Liu, F.; Yang, X.; Feng, H.; Ni, W.; Wang, Y.; Peng, J.; Zhang, H.; Liang, Z.; Yip, H.-L.; Peng, X.; Cao, Y.; Chen, Y. *Nat. Photonics* **2017**, *11*, 85.
- [30] You, J.; Dou, L.; Yoshimura, K.; Kato, T.; Ohya, K.; Moriarty, T.; Emery, K.; Chen, C.-C.; Gao, J.; Li, G.; Yang, Y. *Nat. Commun.* **2013**, *4*, 1446.
- [31] Yusoff, A. R. b. M.; Kim, D.; Kim, H. P.; Shneider, F. K.; da Silva, W. J.; Jang, J. *Energy Environ. Sci.* **2015**, *8*, 303.
- [32] Zheng, Z.; Zhang, S.; Zhang, M.; Zhao, K.; Ye, L.; Chen, Y.; Yang, B.; Hou, J. *Adv. Mater.* **2015**, *27*, 1189.
- [33] Gasparini, N.; Jiao, X.; Heumueller, T.; Baran, D.; Matt, G. J.; Fladischer, S.; Spiecker, E.; Ade, H.; Brabec, C. J.; Ameri, T. *Nat. Energy* **2016**, *1*, 16118.
- [34] Liu, T.; Guo, Y.; Yi, Y.; Huo, L.; Xue, X.; Sun, X.; Fu, H.; Xiong, W.; Meng, D.; Wang, Z.; Liu, F.; Russell, T. P.; Sun, Y. *Adv. Mater.* **2016**, *28*, 10008.
- [35] Liu, T.; Huo, L.; Sun, X.; Fan, B.; Cai, Y.; Kim, T.; Kim, J. Y.; Choi, H.; Sun, Y. *Adv. Energy Mater.* **2016**, *6*, 1502109.
- [36] Lu, H.; Zhang, J.; Chen, J.; Liu, Q.; Gong, X.; Feng, S.; Xu, X.; Ma, W.; Bo, Z. *Adv. Mater.* **2016**, *28*, 9559.
- [37] Nian, L.; Gao, K.; Liu, F.; Kan, Y.; Jiang, X.; Liu, L.; Xie, Z.; Peng, X.; Russell, T. P.; Ma, Y. *Adv. Mater.* **2016**, *28*, 8184.
- [38] Xiao, L.; Gao, K.; Zhang, Y.; Chen, X.; Hou, L.; Cao, Y.; Peng, X. *J. Mater. Chem. A* **2016**, *4*, 5288.
- [39] Nian, L.; Gao, K.; Jiang, Y.; Rong, Q.; Hu, X.; Yuan, D.; Liu, F.; Peng, X.; Russell, T. P.; Zhou, G. *Adv. Mater.* **2017**, *29*, 1700616.
- [40] Cheng, P.; Shi, Q.; Zhan, X. *Acta Chim. Sinica* **2015**, *73*, 252 (in Chinese). (程沛, 史钦钦, 占肖卫, 化学学报, **2015**, *73*, 252.)
- [41] Cheng, P.; Yan, C.; Wu, Y.; Wang, J.; Qin, M.; An, Q.; Cao, J.; Huo, L.; Zhang, F.; Ding, L.; Sun, Y.; Ma, W.; Zhan, X. *Adv. Mater.* **2016**, *28*, 8021.
- [42] Yang, L.; Zhou, H.; Price, S. C.; You, W. *J. Am. Chem. Soc.* **2012**, *134*, 5432.
- [43] Zhang, J.; Zhang, Y.; Fang, J.; Lu, K.; Wang, Z.; Ma, W.; Wei, Z. *J. Am. Chem. Soc.* **2015**, *137*, 8176.
- [44] Zhao, W.; Li, S.; Zhang, S.; Liu, X.; Hou, J. *Adv. Mater.* **2017**, *29*, 1604059.
- [45] Guo, Y.; Zhu, H.; Liu, G.; Yan, H.; Zhu, B.; Li, S.; Sun, Y.; Li, G. *Chin. J. Org. Chem.* **2016**, *36*, 172 (in Chinese). (郭颖, 朱华新, 刘桂林, 严慧敏, 朱冰洁, 李帅, 孙亚军, 李果华, 有机化学, **2016**, *36*, 172.)
- [46] Kadish, K. M.; Smith, K. M.; Guillard, R. *The Porphyrin Handbook: Inorganic, Organometallic and Coordination Chemistry*, Academic Press, San Diego, CA, **1999**.
- [47] Lu, J.; Cai, W.; Zhang, G.; Liu, S.; Ying, L.; Huang, F. *Acta Chim. Sinica* **2015**, *73*, 1153 (in Chinese). (卢俊明, 蔡万清, 张桂传, 刘升建, 应磊, 黄飞, 化学学报, **2015**, *73*, 1153.)
- [48] Gao, K.; Li, L.; Lai, T.; Xiao, L.; Huang, Y.; Huang, F.; Peng, J.; Cao, Y.; Liu, F.; Russell, T. P.; Janssen, R. A. J.; Peng, X. *J. Am. Chem. Soc.* **2015**, *137*, 7282.
- [49] Gao, K.; Miao, J.; Xiao, L.; Deng, W.; Kan, Y.; Liang, T.; Wang, C.; Huang, F.; Peng, J.; Cao, Y.; Liu, F.; Russell, T. P.; Wu, H.; Peng, X. *Adv. Mater.* **2016**, *28*, 4727.
- [50] Liang, T.; Xiao, L.; Gao, K.; Xu, W.; Peng, X.; Cao, Y. *ACS Appl. Mater. Interfaces* **2017**, *9*, 7131.

- [51] Xiao, L.; Chen, S.; Gao, K.; Peng, X.; Liu, F.; Cao, Y.; Wong, W. Y.; Wong, W. K.; Zhu, X. *ACS Appl. Mater. Interfaces* **2016**, *8*, 30176.
- [52] Cheng, P.; Li, Y.; Zhan, X. *Energy Environ. Sci.* **2014**, *7*, 2005.
- [53] He, Y.; Chen, H.-Y.; Hou, J.; Li, Y. *J. Am. Chem. Soc.* **2010**, *132*, 5532.
- [54] Xin, H.; Subramaniyan, S.; Kwon, T. W.; Shoaee, S.; Durrant, J. R.; Jenekhe, S. A. *Chem. Mater.* **2012**, *24*, 1995.
- [55] Li, C. Z.; Chueh, C. C.; Yip, H. L.; O'Malley, K. M.; Chen, W. C.; Jen, A. K. Y. *J. Mater. Chem.* **2012**, *22*, 8574.
- [56] Li, M.; Liu, F.; Wan, X.; Ni, W.; Kan, B.; Feng, H.; Zhang, Q.; Yang, X.; Wang, Y.; Zhang, Y.; Shen, Y.; Russell, T. P.; Chen, Y. *Adv. Mater.* **2015**, *27*, 6296.

(Zhao, X.)